BIOCHEMISTRY
including biophysical chemistry & molecular biology

Article

pubs.acs.org/biochemistry

Temperature Dependence of Internal Motions of Protein Side-Chain NH_3^+ Groups: Insight into Energy Barriers for Transient Breakage of Hydrogen Bonds

Levani Zandarashvili and Junji Iwahara*

Department of Biochemistry and Molecular Biology, Sealy Center for Structural Biology and Molecular Biophysics, University of Texas Medical Branch, Galveston, Texas 77555-1068, United States

Supporting Information

ABSTRACT: Although charged side chains play important roles in protein function, their dynamic properties are not well understood. Nuclear magnetic resonance methods for investigating the dynamics of lysine side-chain NH_3^+ groups were established recently. Using this methodology, we have studied the temperature dependence of the internal motions of the lysine side-chain NH_3^+ groups that form ion pairs with DNA phosphate groups in the HoxD9 homeodomain−DNA complex. For these NH_3^+ groups, we determined order parameters and correlation times for bond rotations and reorientations at 15, 22, 28, and 35 °C. The order parameters were found to be virtually constant in this temperature range. In contrast, the bond-rotation correlation times of the NH_3^+ groups were found to depend strongly on temperature. On the basis of transition state theory, the energy barriers for NH_3^+ rotations were analyzed and compared to those for CH_3 rotations. Enthalpies of activation for NH_3^+ rotations were found to be significantly higher than those for CH_3 rotations, which can be attributed to the requirement of hydrogen bond breakage. However, entropies of activation substantially reduce the overall free energies of activation for NH_3^+ rotations to a level comparable to those for CH_3 rotations. This entropic reduction in energy barriers may accelerate molecular processes requiring hydrogen bond breakage and play a kinetically important role in protein function.

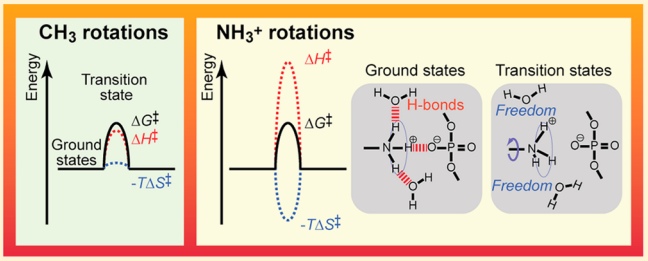

The charged side chains of proteins can form ion pairs and hydrogen bonds that play important roles in protein function. Indeed, their functional significance is evident from numerous three-dimensional structures of enzyme−substrate, protein−protein, and protein−nucleic acid complexes. Nuclear magnetic resonance (NMR) methods for investigating the internal motions of charged side chains of proteins have recently been developed,[1−7] allowing for a substantial deepening of the knowledge of protein dynamics. However, the dynamic properties of hydrogen bonds and/or ion pairs involving protein side chains remain to be delineated, particularly in terms of kinetics and energetics.

The dynamics of hydrogen bonds and ion pairs are relatively well characterized for small ionic compounds in solution. A quarter century ago, rotations of ammonium ions (NH_4^+) in solution were found to occur rapidly on a time scale of $\sim 10^{-12}$ s, although the process should require transient breakage of multiple hydrogen bonds with water molecules.[8,9] *Ab initio* quantum chemical calculations suggest that ~3.2 kcal/mol is required for NH_4^+ to bifurcate one hydrogen bond with water,[10] which gives a simplistic estimate of ~10 kcal/mol for rearranging three hydrogen bonds for NH_4^+ rotation. Nonetheless, the experimental studies showed that solvation imposes an overall barrier of only ~2 kcal/mol for NH_4^+ rotation.[8,9] By time-resolved spectroscopy, it was found that the transitions between the contact ion-pair (CIP) and solvent-separated ion-pair (SIP) states occur on a 10^{-12}−10^{-9} s time scale for ion pairs of small compounds.[11−15] Thus, at least for these small ionic compounds in solution, hydrogen bonds and ion pairs are dynamically broken and formed on a subnanosecond time scale.

Compared to the wealth of information for small compounds, the current knowledge of the dynamics of hydrogen bonding and ion pairing in macromolecules is relatively poor. NMR studies of hydrogen-bond scalar couplings have provided new insight into the hydrogen bonds in proteins and nucleic acids (e.g., reviewed in ref 16). Recently, it was demonstrated that lysine (Lys) side-chain NH_3^+ groups are extremely useful probes for NMR investigations of dynamics involving hydrogen bonds and/or ion pairs relevant to protein functions.[1,2,7,17,18] Bond rotations of protein side-chain NH_3^+ groups forming hydrogen bonds or ion pairs were found to occur on a 10^{-12}−10^{-10} s time scale.[1,2] The rapid NH_3^+ rotations suggest that the breakage of hydrogen bonds occurs rapidly on a subnanosecond time scale, even in the presence of strong short-range electrostatic interactions.

In this work, we gain energetic insight into the dynamics of the Lys side-chain NH_3^+ groups that form ion pairs at the molecular interface of the HoxD9 homeodomain−DNA

Received: October 10, 2014
Revised: December 5, 2014
Published: December 9, 2014

complex. These NH_3^+ groups clearly exhibit $^1H-^{15}N$ correlation signals even at 35 °C,[1,17] a temperature at which observation of NH_3^+ signals is typically difficult because of rapid hydrogen exchange.[18,19] Thus, this system is ideally suited for us to study energy barriers for NH_3^+ groups by investigating the temperature dependence around a physiological range of temperature. We have studied the internal motions of the Lys side-chain NH_3^+ groups at 15, 22, 28, and 35 °C and analyzed the energy barriers for NH_3^+ rotations requiring the transient breakage of hydrogen bonds. Comparison of the energy barriers of NH_3^+ and CH_3 rotations illustrates the unique dynamic properties of hydrogen bonds and ion pairs involving protein side chains.

MATERIALS AND METHODS

Preparation of Protein and DNA. ^2H- and ^{15}N-labeled human HoxD9 homeodomain with a C6S mutation and unlabeled 24 bp DNA were prepared as previously described.[20,21] A 280 μL solution of 0.8 mM complex, 10 mM sodium phosphate (pH 5.8), and 20 mM NaCl was sealed in an inner tube (outer diameter, 4.1 mm) of a 5 mm coaxial NMR tube (Shigemi). D_2O for NMR lock was separately sealed in the thin outer layer of the coaxial tube, which prevents deuteration of the NH_3^+ groups (i.e., $NDH_2^+/ND_2H^+/ND_3^+$ species).

NMR Measurements. NMR relaxation measurements for the Lys NH_3^+ groups of the HoxD9 homeodomain–DNA complex were conducted at 15, 22, 28, and 35 °C using Bruker Avance III spectrometers equipped with cryogenic probes operated at ^1H frequencies of 600 and 800 MHz. ^{15}N longitudinal relaxation rates (R_1), initial transverse relaxation rates ($R_{2,\mathrm{ini}}$), relaxation rates of the $4N_zH_zH_z$ terms $[R(4N_zH_zH_z)]$, and heteronuclear $\{^1H-\}^{15}N$ NOE values were measured for the Lys NH_3^+ groups. The pulse sequences and theoretical details for these NH_3^+ relaxation measurements are given in our previous papers.[2,18] The lengths of the ^{15}N longitudinal relaxation period were 0.04, 0.32, 0.60, 0.88, 1.16, 1.44, 1.72, and 2.0 s, and the repetition delay was 2.1 s in the ^{15}N R_1 experiments. Heteronuclear NOE data for the Lys side-chain NH_3^+ groups were collected as described previously.[1,2,18] The length of the ^1H saturation period in the NOE experiment was 5 s, and the total repetition delays (including the ^1H saturation period) at ^1H frequencies of 800 and 600 MHz were 18 and 12 s, respectively, in the NOE experiments. The $R_{2,\mathrm{ini}}$ rates (i.e., the initial rates for intrinsically biexponential ^{15}N transverse relaxation) of the NH_3^+ groups were measured with seven to nine distinct delays between 4.8 and 105.6 ms, satisfying the criteria described by Esadze et al.[2] The recycle delay for the ^{15}N transverse relaxation experiment was 2.7 s. For the determination of the molecular rotational correlation time (τ_m), backbone ^{15}N R_1 and R_2 relaxation rates were measured at each temperature using the 800 MHz spectrometer. The NMR data were processed with NMRPipe[22] and analyzed with NMRView.[23]

Spectral Density Function and ^{15}N Relaxation for NH_3^+ Groups. Because theoretical details of ^{15}N relaxation of NH_3^+ groups are available in our previous publications,[2,18] here we give a brief description of the spectral density function and analytical forms of ^{15}N relaxation parameters used here. For the dipole–dipole (DD) autorelaxation and DD/DD cross correlation, a general spectral density function for pairs of interacting spins ij and kl in a $^{15}N-^1H_3^+$ system in a macromolecule is given by[2]

$$J_{ijkl}(\omega) = \frac{1}{4\pi}\zeta_{ij}\zeta_{kl}\left\{\frac{S_{\mathrm{f},(ij,kl)}{}^2 S_{\mathrm{axis}}{}^2 \tau_m}{1+\omega^2\tau_m{}^2} + \frac{S_{\mathrm{axis}}{}^2[P_2(\cos\chi_{ij,kl}) - S_{\mathrm{f},(ij,kl)}{}^2]\tau_1}{1+\omega^2\tau_1{}^2} + \frac{S_{\mathrm{f},(ij,kl)}{}^2(1-S_{\mathrm{axis}}{}^2)\tau_2}{1+\omega^2\tau_2{}^2} + \frac{(1-S_{\mathrm{axis}}{}^2)[P_2(\cos\chi_{ij,kl}) - S_{\mathrm{f},(ij,kl)}{}^2]\tau_3}{1+\omega^2\tau_3{}^2}\right\} \quad (1)$$

where $\zeta_{ij} = (6\pi/5)^{1/2}(\mu_0/4\pi)\gamma_i\gamma_j r_{ij}^{-3}$, μ_0 is the vacuum permeability, γ a nuclear gyromagnetic ratio, r_{ij} the distance between spins i and j, $\chi_{ij,kl}$ the angle between the ij and kl vectors, $S_{\mathrm{axis}}{}^2$ a generalized order parameter[24]for the symmetry axis of the AX_3 spin system, $S_{\mathrm{f},(ji,kl)}{}^2$ an order parameter for bond rotation around the symmetry axis, $P_2(x) = (3x^2-1)/2$, τ_m the overall molecular rotational correlation time, $\tau_1^{-1} = \tau_m^{-1} + \tau_f^{-1}$, $\tau_2^{-1} = \tau_m^{-1} + \tau_i^{-1}$, $\tau_3^{-1} = \tau_m^{-1} + \tau_f^{-1} + \tau_i^{-1}$, τ_i a correlation time for reorientation of the symmetry axis, and τ_f a correlation time for bond rotation around the symmetry axis. For autorelaxation, $i = k = \mathrm{N}$ and $j = l = \mathrm{H}$ and the corresponding spectral density is denoted by $J_{\mathrm{auto}}(\omega)$. For N–H/N–H cross correlation, the corresponding spectral density is denoted by $J_{\mathrm{NHNH}}(\omega)$, for which $i = k = \mathrm{N}$, but j and l are different H spins in the spin system. Likewise, the spectral density for H–H/H–N cross correlation is denoted by $J_{\mathrm{HHHN}}(\omega)$, for which $i = j = \mathrm{H}$, k is another H in the AX_3 system, and $l = \mathrm{N}$. $S_{\mathrm{f},(ij,kl)}{}^2$ is given by $P_2(\cos\beta_{ij})P_2(\cos\beta_{kl})$, where β_{ij} is the angle between vector ij and the symmetry axis. It should be noted that the spectral density function eq 1 is valid when both $\tau_i \gg \tau_f$ and $\tau_i \ll \tau_p$, as previously described.[2] Only when $\tau_i \gg \tau_f$ does our spectral density model eq 1 become the same as eq 15 of Kay and Torchia for $^{13}C-^1H_3$ groups.[25] The inequality $\tau_i \gg \tau_f$ does not necessarily hold for NH_3^+ groups because of the presence of a hydrogen bond that may slow the bond rotation.[2] In fact, some NH_3^+ groups exhibit $\tau_i \ll \tau_f$ (see below as well as ref 2). Thus, the spectral density model eq 1 is more appropriate for NH_3^+ groups. On the basis of the covalent geometry for an NH_3^+ group, which is almost ideally tetrahedral even in an ion pair,[26] $S_f^2 = 0.111$ for $J_{\mathrm{auto}}(\omega)$ and $J_{\mathrm{NHNH}}(\omega)$ and $S_f^2 = 0.167$ for $J_{\mathrm{HHHN}}(\omega)$ were used when $S_{\mathrm{axis}}{}^2$, τ_p, and τ_i were determined from the NMR data. With the ^{15}N chemical shift anisotropy (CSA) being as small as 15 ppm,[27] CSA relaxation is negligible for lysine NH_3^+ groups. The DD relaxation terms and their cross correlations govern the ^{15}N relaxation of NH_3^+ groups. ^{15}N longitudinal relaxation rate R_1 of NH_3^+ groups is given by

$$R_1 = 3J_{\mathrm{auto}}(\omega_N) + 6J_{\mathrm{auto}}(\omega_H + \omega_N) + J_{\mathrm{auto}}(\omega_H - \omega_N) \quad (2)$$

The initial rate $R_{2,\mathrm{ini}}$ for intrinsically biexponential ^{15}N transverse relaxation of NH_3^+ groups is given by

$$R_{2,\mathrm{ini}} = 2J_{\mathrm{auto}}(0) + (3/2)J_{\mathrm{auto}}(\omega_N) + 3J_{\mathrm{auto}}(\omega_H + \omega_N) + 3J_{\mathrm{auto}}(\omega_H) + (1/2)J_{\mathrm{auto}}(\omega_H - \omega_N) \quad (3)$$

The heteronuclear NOE for NH_3^+ groups is given by

dx.doi.org/10.1021/bi5012749 | Biochemistry 2015, 54, 538–545

$$\mathrm{NOE} = 1 + 3\left(\frac{\gamma_H}{\gamma_N}\right)\frac{\sigma_{NH}R(4N_zH_zH_z) - 2\Gamma_{NHNH}\Gamma_{HHHN}}{R_1R(4N_zH_zH_z) - 3\Gamma_{NHNH}^2} \quad (4)$$

in which

$$\sigma_{NH} = 2J_{auto}(\omega_H + \omega_N) - (1/3)J_{auto}(\omega_H - \omega_N) \quad (5)$$

$$\Gamma_{NHNH} = 2J_{NHNH}(\omega_N) \quad (6)$$

$$\Gamma_{HHHN} = 2J_{HHHN}(\omega_H) \quad (7)$$

The relaxation rate for $4N_zH_zH_z$ terms is given by

$$R(4N_zH_zH_z) \approx R_1 + 2(\rho_{HH} + k_{ex}^{water}) \quad (8)$$

where ρ_{HH} is the rate of autorelaxation for a ^{1}H nucleus in the AX_3 system via dipole−dipole interactions with external ^{1}H nuclei.[17,28] For NH_3^+ groups, the hydrogen exchange rate k_{ex}^{water} typically dominates in $R(4N_zH_zH_z)$. If the $R(4N_zH_zH_z)$ is much larger than the other rates involved, the heteronuclear NOE becomes

$$\mathrm{NOE} = 1 + 3\left(\frac{\gamma_H}{\gamma_N}\right)\frac{\sigma_{NH}}{R_1} \quad (9)$$

which corresponds to the standard form for the case with no cross correlation involved.

Calculations of Order Parameters, Correlation Times, and Activation Energies. Using ^{15}N R_1, ^{15}N $R_{2,ini}$, heteronuclear NOE, and $R(4N_zH_zH_z)$ data together with eqs 1−7, we determined the order parameter S_{axis}^2 and correlation times τ_i and τ_f for Lys NH_3^+ groups. For the fitting calculations, the following sum of weighted squares for R_1, $R2,ini$, and NOE was minimized:

$$E = \sum\left(\frac{Y_{obs} - Y_{cal}}{Y_{obs}}\right)^2 \quad (10)$$

where Y_{obs} and Y_{cal} stand for observed and calculated quantities, respectively, of R_1, $R_{2,ini}$, and NOE at the ^{1}H frequency of 800 Hz and R_1 and NOE at 600 MHz. The molecular rotational correlation time τ_m and rotational anisotropy $D_\parallel/D_\perp$ at individual temperatures were determined from backbone amide ^{15}N R_1 and R_2 rates.[29,30] The τ_f correlation times for NH_3^+ bond rotations as well as the order parameters S_{axis}^2 and τ_i correlation times for reorientation of the NH_3^+ symmetry axis were calculated with Mathematica (Wolfram) as described previously.[2] Because $R(4N_zH_zH_z)$ rates were far larger than Γ_{NHNH} and Γ_{HHHN} rates, the use of ^{15}N R_1, ^{15}N $R_{2,ini}$, and heteronuclear NOE together with eqs 1−3 and 9 gave virtually the same fitting results. The Arrhenius activation energy (E_a), frequency factor (A), enthalpy of activation ($\Delta H^\ddagger$), and entropy of activation ($\Delta S^\ddagger$) for NH_3^+ rotations were determined from the temperature-dependent τ_f data via nonlinear least-squares fitting with MATLAB (Mathworks).

RESULTS

Temperature Dependence of ^{15}N Relaxation for Lys NH_3^+ Groups. As previously demonstrated,[1,17] the Lys3, Lys55, and Lys57 NH_3^+ groups of the HoxD9 homeodomain−DNA complex at 35 °C exhibited ^{1}H−^{15}N cross-peaks in the ^{1}H−^{15}N heteronuclear in-phase single-quantum correlation (HISQC) spectrum. These side-chain NH_3^+ groups form

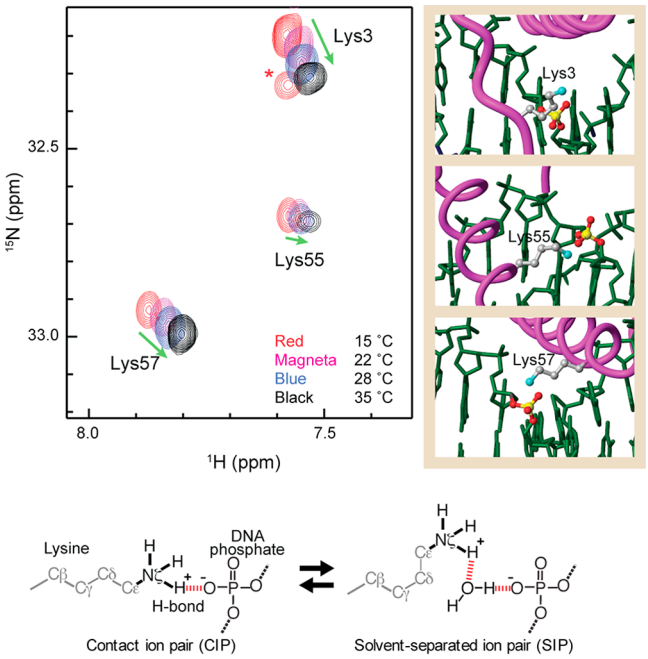

Figure 1. Lys NH_3^+-selective ^{1}H−^{15}N HISQC spectra recorded for the specific complex of ^{2}H- and ^{15}N-labeled HoxD9 homeodomain and 24 bp DNA at 15, 22, 28, and 35 °C. The Lys3, Lys55, and Lys57 NH_3^+ groups are located at the protein−DNA interface and form ion pairs with DNA phosphate groups. A red asterisk indicates a signal from another Lys side chain that can be observed only at a low temperature. The previous NMR study using hydrogen-bond scalar coupling between ^{15}N and ^{13}P nuclei suggested that the major states of these ion pairs are CIP for Lys55 and Lys57 and SIP for Lys3.[1] Locations of these residues in the crystal structures of homeodomain−DNA complexes are also shown (Protein Data Bank entry 1IG7 for Lys3 and Protein Data Bank entry 3HDD for Lys55 and Lys57).

intermolecular ion pairs with DNA phosphate groups. Our previous study using the hydrogen-bond scalar coupling constant between Lys NH_3^+ ^{15}N and DNA phosphate ^{31}P nuclei ($^{h3}J_{NP}$) suggested that the intermolecular ion pairs of Lys55 and Lys57 are mainly in the CIP state, whereas that of Lys3 is mainly in the SIP state.[1] Figure 1 shows the Lys-selective ^{1}H−^{15}N HISQC spectra recorded at 15, 22, 28, and 35 °C. While the Lys3, Lys55, and Lys55 NH_3^+ groups clearly exhibit the HISQC signals, any other NH_3^+ groups of the same protein do not show signals that can be observed above 20 °C because of rapid hydrogen exchange. For the side-chain NH_3^+ groups at the protein−DNA interface, we collected the ^{15}N relaxation data at 15, 22, 28, and 35 °C.

Figure 2 shows the temperature dependence of the ^{15}N relaxation parameters measured for the Lys3, Lys55, and Lys57 NH_3^+ groups at the ^{1}H frequency of 800 MHz. Values of the ^{15}N relaxation parameters measured at ^{1}H frequencies of 600 and 800 MHz are listed in Table S1 of the Supporting Information. As shown in panels A and B of Figure 2, the ^{15}N R_1 and $R_{2,ini}$ rates for these NH_3^+ groups decreased with an increase in temperature. The relaxation rates $R(4N_zH_zH_z)$ significantly increased with an increase in temperature (Figure 2C). As described previously,[1,2] the $R(4N_zH_zH_z)$ rates of NH_3^+ groups are dominated by hydrogen exchange and are roughly equal to twice the hydrogen exchange rate of the NH_3^+ groups. The observed $R(4N_zH_zH_z)$ rates were >50-fold faster than the ^{15}N R_1 rates, ensuring that cross correlation between dipole−dipole relaxation mechanisms is virtually negligible in

dx.doi.org/10.1021/bi5012749 | Biochemistry 2015, 54, 538−545

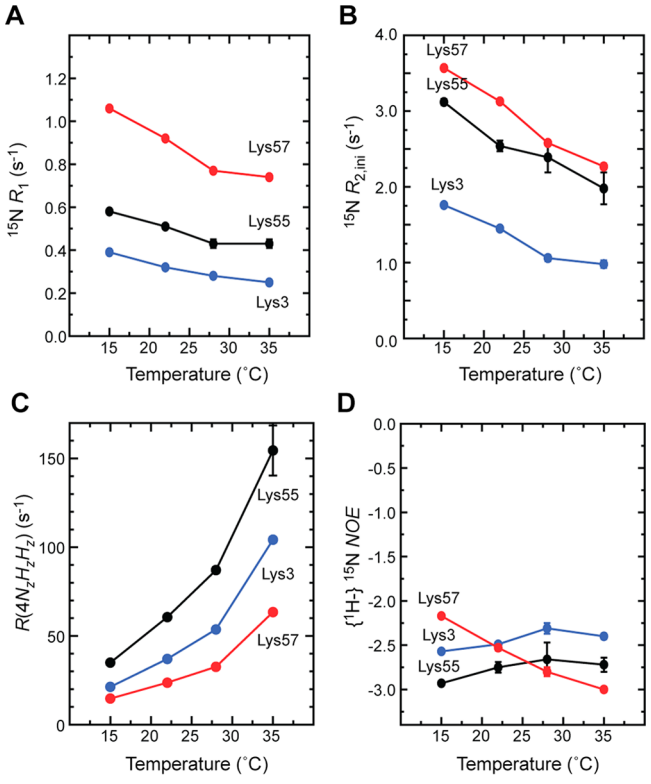

Figure 2. Temperature dependence of ^{15}N relaxation parameters for the side-chain NH_3^+ groups of Lys3 (blue), Lys55 (black), and Lys57 (red) of the HoxD9 homeodomain–DNA complex. (A) ^{15}N longitudinal relaxation rates R_1. (B) Initial rates $R_{2,ini}$ for ^{15}N transverse relaxation. (C) Relaxation rates for $4N_zH_zH_z$ terms. (D) Heteronuclear ^{1}H–^{15}N NOE. The shown data were collected at the ^{1}H frequency of 800 MHz. For ^{15}N R_1 and heteronuclear NOE, we also conducted the NH_3^+ relaxation measurements at the ^{1}H frequency of 600 MHz. Values of these parameters are given in the Supporting Information. For data points with no error bars, uncertainties are smaller than the sizes of the symbols.

heteronuclear NOE measurements for NH_3^+ groups (i.e., eqs 4 and 9 become virtually identical).[2] Heteronuclear NOE values of the Lys3 and Lys55 NH_3^+ groups became larger with an increase in temperature, but the Lys57 NH_3^+ group exhibited an opposite change (Figure 2D), reflecting different motional behaviors for these NH_3^+ groups. The uniqueness in the internal motions of the Lys57 NH_3^+ group became clearer by our further analysis of the bond-rotation and reorientation correlation times, as shown below.

Temperature Dependence of Molecular Rotational Diffusion. The temperature dependence of the ^{15}N relaxation parameters for Lys NH_3^+ groups is partly due to the temperature dependence of the molecular rotational correlation time τ_m. Figure 3 shows the rotational diffusion parameters determined from the protein backbone ^{15}N R_1 and R_2 relaxation rates. The values of τ_m [$=(2D_{\|} + 4D_{\perp})^{-1}$] at 15, 22, 28, and 35 °C were 18.1, 15.3, 12.1, and 10.6 ns, respectively. These results are consistent with the temperature dependence of water viscosity and the Stokes–Einstein relation (yellow curve in Figure 3). The anisotropy of the rotational diffusion ($D_{\|}/D_{\perp}$) was in the range of 2.0–2.2 at these temperatures. This relatively large anisotropy is obviously due to the rod-shaped 24 bp DNA duplex of the complex; in fact, the main principle axis of this diffusion tensor was found to be nearly parallel to the DNA axis (Figure 3). As described previously,[2] the influence of

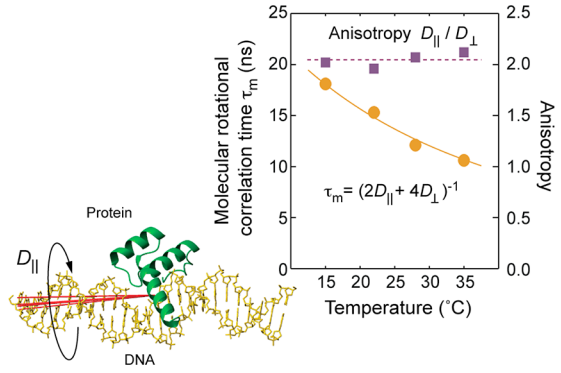

Figure 3. Temperature dependence of the molecular rotational correlation time (circles) and rotational diffusion anisotropy (squares) measured for the specific complex of the HoxD9 homeodomain and 24 bp DNA. An axially symmetric diffusion tensor involving rotational diffusion coefficients $D_{\|}$ and $D_{\perp}$ was used. The shown parameters were determined from the ^{15}N R_1 and R_2 relaxation rates for 44 backbone amide groups in conformationally rigid parts of the complex. The dotted line shows the average of the anisotropy values. The solid line represents the best fit to the theoretical model of τ_m based on the Stokes–Einstein relation and the temperature dependence of water viscosity. Red bars shown together with the structure indicate the main principal axis of the rotational diffusion tensor at the four distinct temperatures.

this rotational anisotropy is virtually negligible for the ^{15}N relaxation of NH_3^+ groups because the small overall order parameters, $S_f^2S_{axis}^2$ ($=0.111S_{axis}^2$), diminish the impact of the rotational anisotropy in the spectral density function.

Temperature Dependence of Order Parameters. Using the ^{15}N relaxation data for the NH_3^+ groups together with the molecular rotational correlation time (τ_m) of the complex at each temperature, we determined order parameters (S_{axis}^2), bond-rotation correlation times (τ_f), and reorientation correlation times (τ_i) for NH_3^+ groups (Figure 4). The model for the internal motions of Lys NH_3^+ groups assumes reorientation of the symmetry axis and Cε–Nζ bond rotations.[2] The order parameter S_{axis}^2 and the correlation time τ_i represent reorientation of the NH_3^+ symmetry axis. Panels A and B of Figure 4 show the temperature dependence of these parameters obtained for the interfacial NH_3^+ groups of the HoxD9 homeodomain–DNA complex. As previously described,[1] these Lys NH_3^+ groups exhibited a high degree of mobility, with S_{axis}^2 values of <0.5, despite the formation of an ion pair with DNA. We found that the order parameters S_{axis}^2 for the Lys NH_3^+ groups were virtually the same in this temperature range (Figure 4A). A similarly weak temperature dependence of order parameters was also reported for the backbone amide and side-chain methyl groups of proteins.[31,32]

Temperature Dependence of Reorientation and Bond-Rotation Correlation Times. Because the presence of hydrogen bonds can substantially slow bond rotations of NH_3^+ groups, it is important that our spectral density model eq 1 can deal with both cases in which $\tau_i \gg \tau_f$ and $\tau_i \ll \tau_f$.[2] Because of this feature of eq 1, however, the function E (eq 10) to be minimized via parameter optimization usually exhibits two minima: one with $\tau_i \gg \tau_f$ and the other with $\tau_i \ll \tau_f$. In most cases, one of the minima is substantially (>50-fold) smaller than the other and clearly represents the global minimum. Our data at 15, 22, and 28 °C showed $\tau_i \gg \tau_f$ for Lys3 and Lys55 and $\tau_i \ll \tau_f$ for Lys57. The unique behavior of the Lys57 NH_3^+ group was also evident from the temperature

dx.doi.org/10.1021/bi5012749 | Biochemistry 2015, 54, 538–545

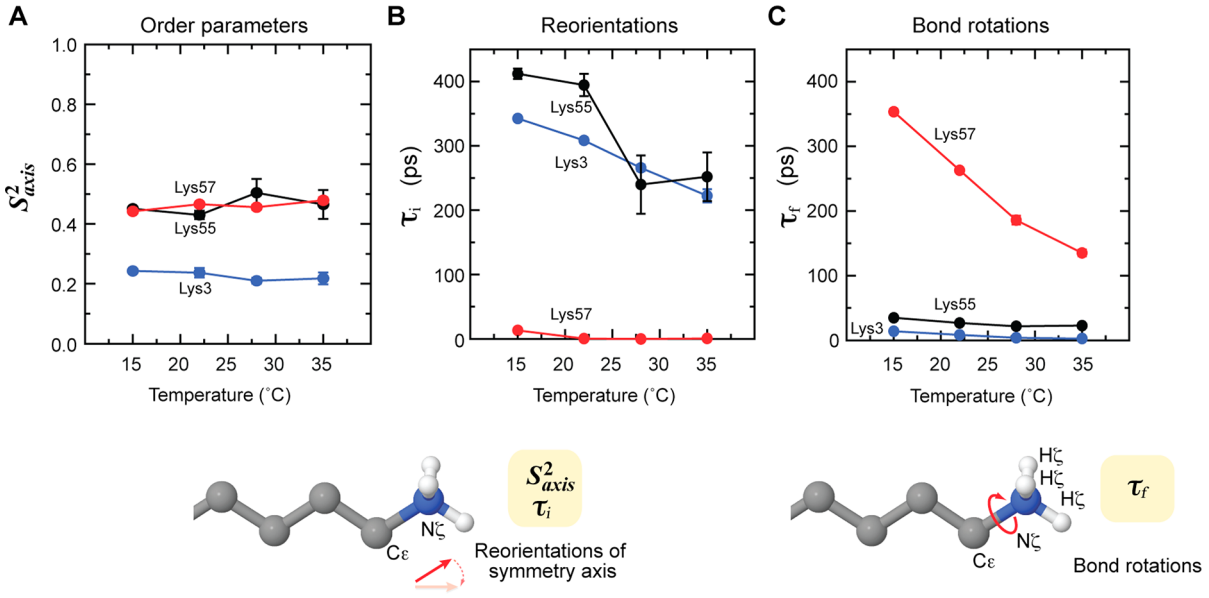

Figure 4. Temperature-dependent internal motions of the Lys3, Lys55, and Lys57 NH_3^+ groups at the molecular interface of the HoxD9 homeodomain−DNA complex. (A) Order parameters $S_{axis}{}^2$ for the symmetry axes of the NH_3^+ groups. (B) Reorientation correlation times τ_i for the NH_3^+ symmetry axes. (C) Bond-rotation correlation times τ_f for the NH_3^+ groups.

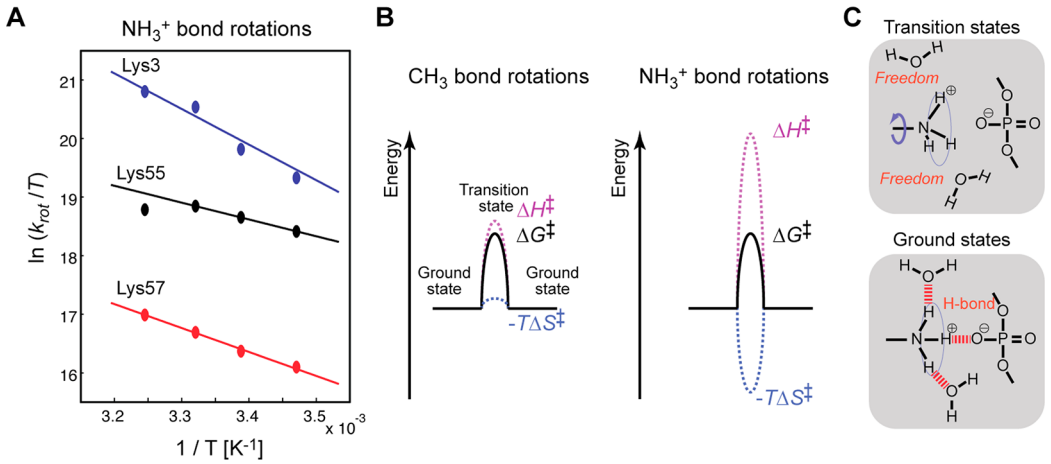

Figure 5. Energy barriers for NH_3^+ bond rotations. (A) Eyring plot of the kinetic rate constants k_{rot} (=$1/\tau_f$) for NH_3^+ bond rotations. Solid lines represent the best-fit curves obtained with the Eyring equation for the experimental data on the Lys3, Lys55, and Lys57 NH_3^+ groups of the HoxD9 homeodomain−DNA complex at 15, 22, 28, and 35 °C. The datum for Lys55 at 35 °C was excluded from the fitting calculations because the quality of the relaxation data for this was not as good as the quality of the others. (B) Schematic representations of the energy barriers for NH_3^+ and CH_3 rotations. (C) Entropically favorable transition states in NH_3^+ bond rotations. Although a large enthalpy of activation is required for the breakage of hydrogen bonds, the transition state gives more freedom to water molecules, thereby resulting in an entropic gain. This can reduce the overall energy barriers ($\Delta G^‡$) for NH_3^+ rotations (see also Table 1).

dependence of heteronuclear NOE (Figure 2D), as mentioned above. During Monte Carlo error estimation for the data of Lys55 and Lys57 at 35 °C, fitting calculations for some synthetic data gave comparable minima for $\tau_i \gg \tau_f$ and $\tau_i \ll \tau_f$ because of relatively large uncertainties in ^{15}N relaxation parameters (note that rapid NH_3^+ hydrogen exchange with water makes the NMR experiments less sensitive at high temperatures). This problem turned out to be the direct cause of large uncertainties in τ_f and τ_i determined in our previous study at 35 °C.[1] To circumvent this problem for Lys57 and Lys55 at 35 °C, we used a constraint of either $\tau_i \gg \tau_f$ or $\tau_i \ll \tau_f$, which was decided on the basis of the results at 15, 22, and 28 °C. This significantly improved the precision in determination of τ_f and τ_i at 35 °C.

The reorientation correlation times (τ_i) were determined less precisely than the other parameters. However, it was still clear that the reorientation correlation times of the Lys3 and Lys55 NH_3^+ groups significantly depended on temperature (Figure 4B). The τ_i values varied between 200 and 450 ps for these NH_3^+ groups, and their reorientations were found to be faster at a higher temperature. The τ_i value of the Lys57 NH_3^+ group was <5 ps, and its temperature dependence was unclear because of low precision.

The values of the bond-rotation correlation times (τ_f) were determined more precisely than the τ_i values. Figure 4C shows the τ_f values for the side-chain NH_3^+ groups at 15, 22, 28, and 35 °C. The Lys57 NH_3^+ group exhibited a τ_f of >100 ps, whereas the Lys3 and Lys55 NH_3^+ groups exhibited τ_f values of

dx.doi.org/10.1021/bi5012749 | Biochemistry 2015, 54, 538−545

<50 ps. On the basis of the crystal structures of homologous homeodomain−DNA complexes,[33,34] we could ascribe the difference in bond rotations of Lys57 and Lys55 NH_3^+ groups to the difference in hydrogen bonds; Lys57 can form hydrogen bonds with DNA phosphate and Met54 Sδ, whereas Lys55 can form hydrogen bonds with only DNA phosphate. Faster bond rotation of the Lys3 NH_3^+ group could be due to a higher degree of exposure to solvent. Base-type-dependent hydration of DNA phosphate[35] might also contribute to the different behaviors of these NH_3^+ groups. Our data showed that the bond-rotation correlation times depended strongly on temperature and were smaller at a higher temperature (Figures 4C and 5A). In fact, the bond rotations of the NH_3^+ groups at 35 °C were ∼2−4 times faster than at 15 °C. To obtain information regarding energy barriers, we conducted further analysis of the NH_3^+ bond rotations, as described below.

Energy Barriers for NH_3^+ Bond Rotations. The correlation time τ_f corresponds to the inverse of the rate constant k_{rot} for C−N bond rotation of 120°. For this kinetic rate constant, we applied the empirical Arrhenius equation as well as the transition state theory-based Eyring equation to our analysis of the energy barriers for NH_3^+ bond rotations. By fitting the temperature-dependent k_{rot} data to the Arrhenius equation, $k = A \exp[-E_a/(RT)]$, we determined the activation energy (E_a) and the frequency factor (A). By using the Eyring equation of transition state theory, $k = [(k_B T)/h] \exp[-\Delta G^{\ddagger}/(RT)] = [(k_B T)/h] \exp(\Delta S^{\ddagger}/R) \exp[-\Delta H^{\ddagger}/(RT)]$, we determined the enthalpy of activation ($\Delta H^{\ddagger}$) and entropy of activation ($\Delta S^{\ddagger}$). Each analysis utilized two fitting parameters (E_a and A for the Arrhenius equation and $\Delta H^{\ddagger}$ and $\Delta S^{\ddagger}$ for the Eyring equation). These equations were found to fit reasonably well to the experimental data. Table 1 summarizes the obtained parameters with regard to the energy barriers of NH_3^+ bond rotations. The values of E_a are in general close to the values of $\Delta H^{\ddagger}$. Figure 5A shows an Eyring plot of the experimental bond-rotation data for each NH_3^+ group together with the best fit with the Eyring equation.

The enthalpies of activation $\Delta H^{\ddagger}$ were significantly larger than the free energies of activation $\Delta G^{\ddagger}$. Interestingly, the values of $\Delta H^{\ddagger}$ for the Lys55 and Lys57 NH_3^+ groups, for which CIP with DNA phosphate is the major state, were smaller than the value of $\Delta H^{\ddagger}$ for the Lys3 NH_3^+ group for which SIP is the major state. This could be attributed to the chaotropic nature of NH_3^+ and the kosmotropic nature of phosphate ions.[36] According to the Collins rule on ion pairs, chaotrope−kosmotrope interactions are enthalpically weaker than water−chaotrope and water−kosmoptrope interactions.[36] Given this rule, the higher $\Delta H^{\ddagger}$ for Lys3 appears to be reasonable because the Lys3 NH_3^+ group, the major state of which is SIP, is likely hydrated by a larger number of water molecules. Despite the larger $\Delta H^{\ddagger}$, the overall $\Delta G^{\ddagger}$ is smaller for the Lys3 NH_3^+ group because of a large entropic $T\Delta S^{\ddagger}$ term, making its bond rotation faster than that of the others. The large $\Delta S^{\ddagger}$ for Lys3 could also be attributed at least partly to the larger number of water molecules that are transiently released by this NH_3^+ group.

Table 1. Activation Energies for Bond Rotations of Protein Side-Chain NH_3^+ and CH_3 Groups

	$\Delta G^{\ddagger}$ (kcal/mol)[a]	$\Delta H^{\ddagger}$ (kcal/mol)[a]	$T\Delta S^{\ddagger}$ (kcal/mol)[a]	E_a (kcal/mol)[b]
NH_3^+ rotations[c]				
HoxD9 Lys3 Nζ	2.1	13.5 ± 2.1	11.3 ± 2.2	15.1 ± 1.2
HoxD9 Lys55 Nζ	3.0	5.7 ± 1.2	2.7 ± 0.8	6.3 ± 1.0
HoxD9 Lys57 Nζ	4.3	8.2 ± 0.5	3.9 ± 0.5	8.6 ± 0.3
CH_3 rotations[d]				
α-spc V9 Cγ1	3.6	2.6 ± 0.3	−1.0 ± 0.3	3.1 ± 0.2
α-spc V58 Cγ2	3.4	3.6 ± 0.3	0.2 ± 0.4	4.0 ± 0.3
α-spc L61 Cδ1	3.0	2.3 ± 0.4	−0.8 ± 0.4	2.7 ± 0.4

[a]Based on transition state theory. Using the Eyring equation, two parameters $\Delta H^{\ddagger}$ and $\Delta S^{\ddagger}$ were optimized in the fitting calculations. The free energy of activation was calculated with the equation $\Delta G^{\ddagger} = \Delta H^{\ddagger} - T\Delta S^{\ddagger}$ together with T = 298 K. Uncertainties were estimated using the Monte Carlo method. [b]Based on the Arrhenius equation: $k = A \exp[-E_a/(RT)]$. Two parameters, E_a and A, were optimized in the fitting calculations. Uncertainties were estimated using the Monte Carlo method. [c]Calculated using the experimental data from this work. [d]Calculated using the experimental data from Figure 2 of ref 44.

DISCUSSION

Comparison to Energy Barriers for CH_3 Bond Rotations. The data from the study presented here allow us to compare energy barriers for protein side-chain CH_3 and NH_3^+ rotations. The methods for investigating the CH_3 dynamics of biological molecules are well-established,[37−39] and activation energies of CH_3 rotations were previously studied by solution NMR as well as by solid state NMR.[40−44] Under conditions near room temperature, the bond-rotation correlation times for CH_3 groups are typically on the order of 10^{-12}−10^{-10} s, with an activation energy E_a in the range of 2−4 kcal/mol. Using solution NMR spectroscopy, Xue et al. measured bond-rotation correlation times τ_f for protein side-chain CH_3 groups at 10, 17, 24, and 30 °C and determined activation energies for CH_3 bond rotations.[44] Table 1 includes the activation energies E_a from their paper as well as the enthalpies and entropies of activation we calculated from their representative data for the Val9 γ1, V58 γ2, and Leu61 δ1 CH_3 groups of the α-spc SH3 domain.

The free energies of activation $\Delta G^{\ddagger}$ for CH_3 and NH_3^+ rotations are comparable, resulting in a similar time scale of bond rotations. However, the enthalpies of activation for NH_3^+ rotations are higher by 2−10 kcal/mol than those for CH_3 rotations. The higher enthalpies of activation for NH_3^+ rotations can be attributed to the presence of hydrogen bonds that need to be transiently broken for rotations. The observed enthalpies of activation for NH_3^+ rotations are at least qualitatively consistent with the Collins rule[36] (see above) as well as with the *ab initio* calculations of energies to bifurcate the hydrogen bonds of a hydrated NH_4^+ ion.[10] The large enthalpies of activation are offset by the large entropy of activation for NH_3^+ bond rotations. In contrast, this enthalpy−entropy compensation in the energy barrier is absent for CH_3 rotations because the entropic term $T\Delta S^{\ddagger}$ for CH_3 rotations is much smaller or even negative (Table 1). The characteristic differences between the energy barriers for NH_3^+ and CH_3 rotations are schematically depicted in Figure 5B.

Entropically Favorable Transition States in NH_3^+ Rotations. This study demonstrates that a positive and large entropic term $T\Delta S^{\ddagger}$ compensates for a large $\Delta H^{\ddagger}$ term and lowers the overall energy barrier $\Delta G^{\ddagger}$ for NH_3^+ bond rotations.

dx.doi.org/10.1021/bi5012749 | *Biochemistry* 2015, 54, 538−545

This enthalpy−entropy compensation appears to be the major reason why bond rotations of NH_3^+ groups can occur nearly as rapidly as the rotations of CH_3 groups, despite the presence of hydrogen bonds. How can the transition states be entropically favorable in NH_3^+ bond rotations? We speculate that the transient breakage of hydrogen bonds could give more freedom to the water molecules, resulting in an entropic gain of the system in the transition state (Figure 5C). In fact, ions are known to restrict water molecules via *electrostriction*, which leads to a reduction in entropy.[45] For some ions, entropic gain due to the release of water molecules is known to be the driving force in their ion-pair formations.[46] The energy barrier between the CIP and SIP states of NaCl in solution also involves strong enthalpy−entropy compensation arising from water molecules.[47] A positive $T\Delta S^{\ddagger}$ is also known for the breakage of nonionic hydrogen bonds involving water molecules.[48] The enthalpy−entropy compensation arising from a decrease in the electrostriction of water molecules might be a general mechanism that accelerates processes involving hydrogen bonds or ion pairs.

Biological Implication. This entropic reduction in energy barriers for breaking hydrogen bonds may be biologically significant because there are many biological molecular processes that require rapid breakage of hydrogen bonds and ion pairs. For example, for rapid turnover of enzymatic reactions, enzymes have to break hydrogen bonds with products and release them from their active site upon completion of the catalytic reaction. When transcription factors such as HoxD9 search for their target sites on DNA, they stochastically scan DNA through nonspecific association. Rapid breakage of Lys/Arg−phosphate ion pairs should be necessary for the proteins to rapidly transfer one nonspecific site to another on DNA.[49]

Concluding Remarks. In this work, we have shown the temperature dependence of the internal motions of protein side-chain NH_3^+ groups forming intermolecular ion pairs with DNA. For these NH_3^+ groups, the order parameters were found to be virtually constant in the temperature range between 15 and 35 °C, whereas the bond-rotation and reorientation correlation times were found to significantly depend on temperature. Our data for the HoxD9 homeodomain−DNA complex clearly show that the enthalpies of activation for NH_3^+ bond rotations are relatively large, most likely because of the requirement of transient hydrogen-bond breakage. The large enthalpies of activation are offset by the entropic gain in the transition states. The entropic reduction in the overall energy barrier might be due to freedom arising from transient breakage of hydrogen bonds between NH_3^+ and water in the transition states. Because of this enthalpy−entropy compensation that greatly lowers the energy barriers, the NH_3^+ groups can undergo rapid bond rotations on a subnanosecond time scale, even though the rotations require transient breakage of hydrogen bonds. This entropic reduction in energy barriers for breaking hydrogen bonds may play a kinetically important role in protein function.

■ ASSOCIATED CONTENT

Supporting Information

A table of $^{15}NH_3^+$ relaxation parameters measured at ^1H frequencies of 800 and 600 MHz. This material is available free of charge via the Internet at http://pubs.acs.org.

■ AUTHOR INFORMATION

Corresponding Author

*Address: 301 University Blvd., Galveston, TX 77555-1068. E-mail: j.iwahara@utmb.edu. Phone: (409) 747-1403.

Funding

This work was supported by National Science Foundation Grant CHE-1307344.

Notes

The authors declare no competing financial interest.

■ ACKNOWLEDGMENTS

We thank Dr. Montgomery Pettitt for useful discussions and Dr. Tianzhi Wang for maintenance of the NMR facility of the University of Texas Medical Branch.

■ ABBREVIATIONS

CIP, contact ion pair; DD, dipole−dipole; HISQC, heteronuclear in-phase single-quantum coherence; NOE, nuclear Overhauser enhancement; SIP, solvent-separated ion pair.

■ REFERENCES

(1) Anderson, K. M., Esadze, A., Manoharan, M., Bruschweiler, R., Gorenstein, D. G., and Iwahara, J. (2013) Direct Observation of the Ion-Pair Dynamics at a Protein-DNA Interface by NMR Spectroscopy. *J. Am. Chem. Soc. 135*, 3613−3619.

(2) Esadze, A., Li, D. W., Wang, T., Brüschweiler, R., and Iwahara, J. (2011) Dynamics of lysine side-chain amino groups in a protein studied by heteronuclear ^1H-^{15}N NMR spectroscopy. *J. Am. Chem. Soc. 133*, 909−919.

(3) Paquin, R., Ferrage, F., Mulder, F. A., Akke, M., and Bodenhausen, G. (2008) Multiple-timescale dynamics of side-chain carboxyl and carbonyl groups in proteins by ^{13}C nuclear spin relaxation. *J. Am. Chem. Soc. 130*, 15805−15807.

(4) Stafford, K. A., Ferrage, F., Cho, J. H., and Palmer, A. G. (2013) Side Chain Dynamics of Carboxyl and Carbonyl Groups in the Catalytic Function of *Escherichia coli* Ribonuclease H. *J. Am. Chem. Soc. 135*, 18024−18027.

(5) Trbovic, N., Cho, J. H., Abel, R., Friesner, R. A., Rance, M., and Palmer, A. G., III (2009) Protein side-chain dynamics and residual conformational entropy. *J. Am. Chem. Soc. 131*, 615−622.

(6) Werbeck, N. D., Kirkpatrick, J., and Hansen, D. F. (2013) Probing Arginine Side-Chains and Their Dynamics with Carbon-Detected NMR Spectroscopy: Application to the 42 kDa Human Histone Deacetylase 8 at High pH. *Angew. Chem., Int. Ed. 52*, 3145−3147.

(7) Zandarashvili, L., Li, D. W., Wang, T., Brüschweiler, R., and Iwahara, J. (2011) Signature of mobile hydrogen bonding of lysine side chains from long-range ^{15}N-^{13}C scalar J-couplings and computation. *J. Am. Chem. Soc. 133*, 9192−9195.

(8) Perrin, C. L., and Gipe, R. K. (1986) Rotation, Solvation, and Hydrogen-Bonding of Aqueous Ammonium Ion. *J. Am. Chem. Soc. 108*, 1088−1089.

(9) Perrin, C. L., and Gipe, R. K. (1987) Rotation and solvation of ammonium ion. *Science 238*, 1393−1394.

(10) Kassab, E., Evleth, E. M., and Hamou-Tahra, Z. D. (1990) Theoretical characterization of the rotational motion of NH_4^+ in water clusters. *J. Am. Chem. Soc. 112*, 103−108.

(11) Lü, J. M., Rosokha, S. V., Lindeman, S. V., Neretin, I. S., and Kochi, J. K. (2005) "Separated" versus "contact" ion-pair structures in solution from their crystalline states: Dynamic effects on dinitrobenzenide as a mixed-valence anion. *J. Am. Chem. Soc. 127*, 1797−1809.

(12) Masnovi, J. M., and Kochi, J. K. (1985) Direct Observation of Ion-Pair Dynamics. *J. Am. Chem. Soc. 107*, 7880−7893.

(13) Peters, K. S., and Li, B. L. (1994) Picosecond Dynamics of Contact Ion-Pairs and Solvent-Separated Ion-Pairs in the Photosolvolysis of Diphenylmethyl Chloride. *J. Phys. Chem. 98*, 401−403.

(14) Simon, J. D., and Peters, K. S. (1982) Picosecond Dynamics of Ion-Pairs: The Effect of Hydrogen-Bonding on Ion-Pair Intermediates. *J. Am. Chem. Soc. 104*, 6542−6547.
(15) Yabe, T., and Kochi, J. K. (1992) Contact Ion-Pairs: Picosecond Dynamics of Solvent Separation, Internal Return, and Special Salt Effect. *J. Am. Chem. Soc. 114*, 4491−4500.
(16) Grzesiek, S., Cordier, F., Jaravine, V., and Barfield, M. (2004) Insights into biomolecular hydrogen bonds from hydrogen bond scalar couplings. *Prog. NMR Spectrosc. 45*, 275−300.
(17) Iwahara, J., Jung, Y. S., and Clore, G. M. (2007) Heteronuclear NMR spectroscopy for lysine NH_3 groups in proteins: Unique effect of water exchange on ^{15}N transverse relaxation. *J. Am. Chem. Soc. 129*, 2971−2980.
(18) Zandarashvili, L., Esadze, A., and Iwahara, J. (2013) NMR studies on the dynamics of hydrogen bonds and ion pairs involving lysine side chains of proteins. *Adv. Protein Chem. Struct. Biol. 93*, 37−80.
(19) Esadze, A., Zandarashvili, L., and Iwahara, J. (2014) Effective strategy to assign ^{1}H-^{15}N heteronuclear correlation NMR signals from lysine side-chain NH_3^+ groups of proteins at low temperature. *J. Biomol. NMR 60*, 23−27.
(20) Iwahara, J., and Clore, G. M. (2006) Direct observation of enhanced translocation of a homeodomain between DNA cognate sites by NMR exchange spectroscopy. *J. Am. Chem. Soc. 128*, 404−405.
(21) Iwahara, J., Zweckstetter, M., and Clore, G. M. (2006) NMR structural and kinetic characterization of a homeodomain diffusing and hopping on nonspecific DNA. *Proc. Natl. Acad. Sci. U.S.A. 103*, 15062−15067.
(22) Delaglio, F., Grzesiek, S., Vuister, G. W., Zhu, G., Pfeifer, J., and Bax, A. (1995) NMRPipe: A Multidimensional Spectral Processing System Based on Unix Pipes. *J. Biomol. NMR 6*, 277−293.
(23) Johnson, B. A., and Blevins, R. A. (1994) Nmr View: A Computer-Program for the Visualization and Analysis of NMR Data. *J. Biomol. NMR 4*, 603−614.
(24) Lipari, G., and Szabo, A. (1982) Model-Free Approach to the Interpretation of Nuclear Magnetic-Resonance Relaxation in Macromolecules. 1. Theory and Range of Validity. *J. Am. Chem. Soc. 104*, 4546−4559.
(25) Kay, L. E., and Torchia, D. A. (1991) The Effects of Dipolar Cross-Correlation on C-13 Methyl-Carbon T1, T2, and NOE Measurements in Macromolecules. *J. Magn. Reson. 95*, 536−547.
(26) Lehmann, M. S., Koetzle, T. F., and Hamilton, W. C. (1972) Precision neutron diffraction structure determination of protein and nucleic acid components. I. The crystal and molecular structure of the amino acid L-alanine. *J. Am. Chem. Soc. 94*, 2657−2660.
(27) Sarkar, S. K., Hiyama, Y., Niu, C. H., Young, P. E., Gerig, J. T., and Torchia, D. A. (1987) Molecular dynamics of collagen side chains in hard and soft tissues. A multinuclear magnetic resonance study. *Biochemistry 26*, 6793−6800.
(28) Skrynnikov, N. R., and Ernst, R. R. (1999) Detection of intermolecular chemical exchange through decorrelation of two-spin order. *J. Magn. Reson. 137*, 276−280.
(29) Iwahara, J., Peterson, R. D., and Clubb, R. T. (2005) Compensating increases in protein backbone flexibility occur when the dead ringer AT-rich interaction domain (ARID) binds DNA: A nitrogen-15 relaxation study. *Protein Sci. 14*, 1140−1150.
(30) Tjandra, N., Feller, S. E., Pastor, R. W., and Bax, A. (1995) Rotational diffusion anisotropy of human ubiquitin from N-15 NMR relaxation. *J. Am. Chem. Soc. 117*, 12562−12566.
(31) Lee, A. L., Sharp, K. A., Kranz, J. K., Song, X. J., and Wand, A. J. (2002) Temperature dependence of the internal dynamics of a calmodulin-peptide complex. *Biochemistry 41*, 13814−13825.
(32) Mandel, A. M., Akke, M., and Palmer, A. G., III (1996) Dynamics of ribonuclease H: Temperature dependence of motions on multiple time scales. *Biochemistry 35*, 16009−16023.
(33) Fraenkel, E., and Pabo, C. O. (1998) Comparison of X-ray and NMR structures for the Antennapedia homeodomain-DNA complex. *Nat. Struct. Biol. 5*, 692−697.
(34) Longo, A., Guanga, G. P., and Rose, R. B. (2007) Structural basis for induced fit mechanisms in DNA recognition by the Pdx1 homeodomain. *Biochemistry 46*, 2948−2957.
(35) Schneider, B., Patel, K., and Berman, H. M. (1998) Hydration of the phosphate group in double-helical DNA. *Biophys. J. 75*, 2422−2434.
(36) Collins, K. D. (1997) Charge density-dependent strength of hydration and biological structure. *Biophys. J. 72*, 65−76.
(37) Ruschak, A. M., and Kay, L. E. (2010) Methyl groups as probes of supra-molecular structure, dynamics and function. *J. Biomol. NMR 46*, 75−87.
(38) Sheppard, D., Sprangers, R., and Tugarinov, V. (2010) Experimental approaches for NMR studies of side-chain dynamics in high-molecular-weight proteins. *Prog. NMR Spectrosc. 56*, 1−45.
(39) Tugarinov, V., and Kay, L. E. (2005) Methyl groups as probes of structure and dynamics in NMR studies of high-molecular-weight proteins. *ChemBioChem 6*, 1567−1577.
(40) Batchelder, L. S., Niu, C. H., and Torchia, D. A. (1983) Methyl Reorientation in Polycrystalline Amino-Acids and Peptides: A H-2 NMR Spin-Lattice Relaxation Study. *J. Am. Chem. Soc. 105*, 2228−2231.
(41) Beshah, K., and Griffin, R. G. (1989) Deuterium Quadrupole Echo NMR-Study of Methyl-Group Dynamics in N-Acetyl-Dl-(γ-D6)-Valine. *J. Magn. Reson. 84*, 268−274.
(42) Copie, V., Mcdermott, A. E., Beshah, K., Williams, J. C., Spijkerassink, M., Gebhard, R., Lugtenburg, J., Herzfeld, J., and Griffin, R. G. (1994) Deuterium Solid-State Nuclear-Magnetic-Resonance Studies of Methyl-Group Dynamics in Bacteriorhodopsin and Retinal Model Compounds: Evidence for a 6-S-Trans Chromophore in the Protein. *Biochemistry 33*, 3280−3286.
(43) Keniry, M. A., Kintanar, A., Smith, R. L., Gutowsky, H. S., and Oldfield, E. (1984) Nuclear magnetic resonance studies of amino acids and proteins. Deuterium nuclear magnetic resonance relaxation of deuteriomethyl-labeled amino acids in crystals and in *Halobacterium halobium* and *Escherichia coli* cell membranes. *Biochemistry 23*, 288−298.
(44) Xue, Y., Pavlova, M. S., Ryabov, Y. E., Reif, B., and Skrynnikov, N. R. (2007) Methyl rotation barriers in proteins from ^{2}H relaxation data. Implications for protein structure. *J. Am. Chem. Soc. 129*, 6827−6838.
(45) Laidler, K. J. (1987) Reactions between ions. In *Chemical Kinetics*, pp 191−202, Longman, New York.
(46) Marcus, Y., and Hefter, G. (2006) Ion pairing. *Chem. Rev. 106*, 4585−4621.
(47) Pettitt, B. M., and Rossky, P. J. (1986) Alkali-Halides in Water: Ion Solvent Correlations and Ion Ion Potentials of Mean Force at Infinite Dilution. *J. Chem. Phys. 84*, 5836−5844.
(48) van der Spoel, D., van Maaren, P. J., Larsson, P., and Timneanu, N. (2006) Thermodynamics of hydrogen bonding in hydrophilic and hydrophobic media. *J. Phys. Chem. B 110*, 4393−4398.
(49) Esadze, A., Kemme, C. A., Kolomeisky, A. B., and Iwahara, J. (2014) Positive and negative impacts of nonspecific sites during target location by a sequence-specific DNA-binding protein: Origin of the optimal search at physiological ionic strength. *Nucleic Acids Res. 42*, 7039−7046.